A&A 413, 693–709 (2004)
DOI: 10.1051/0004-6361:20031463

Astronomy & Astrophysics

Bright OB stars in the Galaxy

I. Mass-loss and wind-momentum rates of O-type stars: A pure Hα analysis accounting for line-blanketing

N. Markova[1], J. Puls[2], T. Repolust[2], and H. Markov[1]

[1] Institute of Astronomy and Isaac Newton Institute of Chile Bulgarian Branch, Bulgarian National Astronomical Observatory, PO Box 136, 4700 Smoljan, Bulgaria
e-mail: rozhen@mbox.digsys.bg
[2] Universitäts-Sternwarte München, Scheinerstrasse 1, 81679 Munchen, Germany

Received 20 December 2002 / Accepted 11 September 2003

Abstract. We study mass-loss and wind momentum rates of 29 Galactic O-type stars with luminosity classes I, III and V by means of a pure Hα profile analysis and investigate to what extent the results compare to those originating from a state-of-the-art, complete spectral analysis. Our investigation relies on the approximate method developed by Puls et al. (1996) which we have modified to account for the effects of line-blanketing. Effective temperatures and gravities needed to obtain *quantitative* results from such a simplified approach have been derived by means of calibrations based on most recent spectroscopic NLTE analyses and models of Galactic stars by Repolust et al. (2003) and Martins et al. (2002). Comparing (i) the derived wind-densities to those determined by Repolust et al. (2003) for eleven stars in common and (ii) the Wind-momentum Luminosity Relationship (WLR) for our sample stars to those derived by other investigations, we conclude that our approximate approach is actually able to provide consistent results. Additionally, we studied the consequences of "fine tuning" some of the direct and indirect parameters entering the WLR, especially by accounting for different possible values of stellar reddening and distances. Combining our data set with the corresponding data provided by Herrero et al. (2002) and Repolust et al. (2003) we finally study the WLR for the largest sample of Galactic O-type stars gathered so far, including an elaborate error treatment. The established disagreement between the theoretical predictions and the "observed" WLRs being a function of luminosity class is suggested to be a result of wind clumping. Different strategies to check this hypothesis are discussed, particularly by comparing the Hα mass-loss rates with the ones derived from radio observations.

Key words. stars: early-type – stars: mass-loss – stars: winds, outflows – stars: distances – stars: fundamental parameters

1. Introduction

The evolution of the Universe, since the time when the first stars were formed, is a central topic of present-day astrophysical research. Massive stars are the main engines which drive this cosmic evolution. Although rotation may also play an important role, mass-loss is still considered to be the dominant process for the evolution of these stars. As shown in numerous stellar evolution calculations, a change in mass-loss rates of massive stars by even a factor of 2 has a dramatic effect on their evolution (Meynet et al. 1994). Indeed, the nature of the eventual supernova explosion may depend critically on the precursor's mass-loss history, in particular during the poorly understood post main-sequence phases of evolution (Woosley et al. 2002).

Thus, accurate mass-loss rates are crucial for both our knowledge of the nature and evolution of massive stars and our understanding of the Universe as a whole. Accurate mass-loss rates are also important with respect to the so-called Wind-momentum Luminosity Relationship (WLR, cf. Kudritzki & Puls 2000, and references therein) which will provide an alternative possibility to determine extragalactic distances by means of purely spectroscopic tools. There are several physical processes that may effect and significantly modify the observed mass-loss rates, of which the most important are metallicity, wind clumping, spectral variability and rotation.

During the recent years new model atmosphere codes have been developed which can provide accurate and consistent stellar and wind parameters for O-type stars. These codes take the effects of NLTE and winds properly into account, in particular the presence of metal line-blocking/blanketing (Hillier & Miller 1998; Pauldrach et al. 2001; Herrero et al. 2002). The inclusion of these processes has a strong impact on the derived

Send offprint requests to: N. Markova,
e-mail: markova@usm.uni-muenchen.de

effective temperatures and leads to lower values, compared to results from unblanketed models (Martins et al. 2002; Herrero et al. 2002; Crowther et al. 2002; Bianchi & Garcia 2002; Repolust et al. 2003), see also Hubeny & Lanz (1995). This temperature reduction leads to a downward revision of stellar luminosities (and, to a lesser extent, of gravities, radii and mass-loss rates) for O-type stars.

The application of the new codes, in particular to far-UV and UV spectra, indicated that O-star winds might be clumped (Crowther et al. 2002; Bianchi & Garcia 2002; Massa et al. 2003), which is in agreement with predictions from time-dependent hydrodynamical simulations (Owocki et al. 1988; Feldmeier 1995; Owocki & Puls 1999). Additional evidence in support of the clumped nature of O-star winds has been found by Repolust et al. (2003, henceforth "RPH") who studied the corresponding WLR using optical spectra. These authors confirmed the clear separation between the WLRs for luminosity class I (lc I) and luminosity class III/V (lc III/V) stars, already detected by means of unblanketed analyses (Puls et al. 1996). Note that such a separation is in contrast to present-day theoretical simulations of line-driven winds, predicting a unique relation instead (Vink et al. 2000; Pauldrach et al. 2002; Puls et al. 2003).

The effect of clumping may be the key to resolve this discrepancy. In particular, Puls et al. (2003) suggested that there might be no separation at all, but that one can "see" the effects of clumping in objects with Hα in emission (i.e., with a large contributing wind volume), which then mimics a higher mass-loss rate (and thus wind-momentum) than actually present. In objects with Hα in absorption, on the other hand, only contributions from the innermost (not clumped) wind are present and, thus, $\dot{M}$ is observed at its actual value.

The possibility to use the WLR of O-stars as an indicator of wind clumping is very exciting but still needs to be proven. One way to check this possibility is to compare mass-loss rates derived from wind diagnostics relying on different density dependences, e.g., from Hα and UV resonance lines. In fact, a coarse comparison of observed and synthetic UV spectra performed by Puls et al. (2003) revealed that for those objects where the Hα mass-loss rates did not agree with the theoretical predictions, SiIV (which is ρ^2-dependent) favoured the "observed", i.e., larger mass-loss rate. Those lines, however, which form close to the photosphere seemed to be consistent with a lower value. Hence, a (re-)analysis of UV spectra aiming at an independent $\dot{M}$ determination for those stars with Hα in emission might by worthwhile.

Another possibility to check for clumping in O-star winds is to compare Hα and radio mass-loss rates. In the case of completely clumped winds and owing to the suggested radial stratification of the clumping factor (Owocki et al. 2000), radio and Hα mass-loss rates might differ significantly. The comparisons performed so far do not give evidence of any systematic difference (Lamers & Leitherer 1993; Scuderi & Panagia 2000). Note, however, that in view of the interpretation by Puls et al. (2003) also this result needs to be re-investigated (cf. Sect. 6).

Following the outlined reasoning, we have started a project to address the questions of wind clumping in O-type stars (beginning with Galactic objects), by comparison of optical data with radio (and IR) mass-loss rates. Such a project requires a (very) large sample of stars to be analyzed, because of the rather large error bars in $\dot{M}$-estimates for individual objects (at least in our Galaxy, due to uncertain distances). It must be noted, however, that the computational effort to analyze the spectra of even *one* star is extremely large, so that the application of the codes mentioned above becomes rather problematic.

In order to find a suitable resolution to this problem, we decided to investigate the following question: to what extent can the analysis of the Hα profile *alone* provide results consistent with those originating from a complete spectral analysis? In case of reasonable agreement, such an analysis can be used at least in two ways: first, valuable information can be added to complement smaller samples which have been analyzed in a detailed way by using already available Hα spectra (or spectra with missing strategic lines). Second, from such an analysis targets for follow-up observations (and analyses) can be selected, particularly for investigations in the radio and IR band.

The results of this investigation are presented in the following. In Sects. 2 and 3 we describe the observational material and the stellar sample; in Sect. 4 we outline the method, determine mass-loss rates and compare with results from complete analyses. Based on these data and as a first application we derive the corresponding WLR and compare it with similar studies as shown in Sect. 5. Having convinced ourselves that the simplified approach gives consistent results, we finally combine our data with alternative data sets, namely those from RPH and Herrero et al. (2002), to obtain the largest sample of Galactic O-stars used so far for a study of the WLR. In Sect. 6 we discuss the implications and present our (preliminary) conclusions.

2. Spectral observations

The Hα spectra analyzed in the present work have been obtained as part of a three year observation program to study wind variability of luminous early type stars in our Galaxy. We used the Coudé spectrograph of the 2m RCC telescope at the National Astronomical Observatory, Bulgaria. The project started in 1997 with an ELECTRON CCD with 520×580 pixels of $22 \times 24\ \mu$ as detector. Beginning in the fall of 1998, we used a PHOTOMETRIC CCD with a pixel area of 1024×1024 and a pixel size of $24\ \mu$. With the former configuration approximately 115 Å can be observed in one exposure with a resolution of $R = 15\,000$, while with the latter one the spectrum coverage is approximately 200 Å, again with a resolution of 15 000. Spectra taken in April 1998 were obtained using a SBIG ST6 Thomson CCD with an area of 375×242 pixels and a pixel size of $23 \times 27\ \mu$. The resolution of these spectra is 15 000 over a spectral range of 72 Å.

While the observational material derived throughout this program has been/will be used as a basis for a series of investigations dealing with wind variability itself, in the present study we have considered only one (the most "representative") spectrum per star.

We followed a standard procedure for data reduction, including bias subtraction, flat-fielding, cosmic ray hits removal, wavelength calibration and correction for heliocentric radial

velocity. The spectra were normalized by a polynomial fit to the continuum, specified by carefully selected continuum windows, and re-binned to a step-size of 0.2 Å per pixel. The atmospheric water vapour lines were removed by dividing each spectrum of each target with a specially constructed "telluric spectrum". All steps in the reduction procedure were performed using a series of modules written in IDL. More information about the observations and the reduction procedure can be found in Markova & Valchev (2000).

3. Sample stars

Our sample consists of 29 stars with spectral classes ranging from O4 to O9.7 including 22 supergiants of luminosity class If, Ia, Ib and Iab, one bright giant, 3 normal giants and 3 dwarfs. The stars are listed in Table 1 together with the adopted spectral types and luminosity classes (Col. 2), clusters or association membership (Col. 3), visual magnitudes and $(B-V)$ colours (Cols. 4 and 5), extinction ratio R and distances (Cols. 6 and 7) and absolute magnitudes, M_V (Col. 8).

Twenty one of the targets have been selected by means of the following criteria:

- to be brighter than 9^m in order to allow spectra with a signal-to-noise ratio of approximately 200 to be obtained with the available instruments in less than 15 min;
- to be spectroscopically single stars (see below);
- to be members of clusters or associations, i.e., to have "known" distances.

The remaining eight targets (displayed in the lower part of Table 1) satisfy the first two criteria but are not members of clusters or associations. Nevertheless, we have included these stars into our sample because, first, they have never been analyzed with respect to mass-loss rates using Hα (except for HD 188 209). Second, a part of them has recently been observed as radio sources (Scuderi et al. 2003), whereas the other part has good chances to be detected in the radio band as their Hα profiles appear mainly in emission. In particular, we intend to use these additional objects in order to derive constraints on the clumpiness of their winds.

Spectral types and luminosity classes for the majority of the stars are taken from the work of Walborn (1971, 1972, 1973). For HD 24 912, however, we adopt a luminosity class I instead of III as assigned by Walborn, in agreement with Herrero et al. (1992) who found that even with the correction for the effects of centrifugal forces the gravity of this star is much lower than for typical luminosity class III objects. For the two stars without a classification by Walborn, BD+56739 and HD 338 926, spectral types and luminosity classes originate from Hiltner (1956) and from Hiltner & Iriarte (1955), respectively.

Cluster and association membership are from Humphreys (1978), from Garmany & Stencel (1992) and from Lennon et al. (1992, HD 30 614). For all but two stars, HD 66 811 and HD 30 614, distances adopted by Humphreys (1978) have been used. In these two exceptional cases, distances are taken from the Galactic O Stars Catalogue (Cruz-Gonzalez et al. 1974). To check the stars for spectroscopic binarity we consulted the list of Gies (1987).

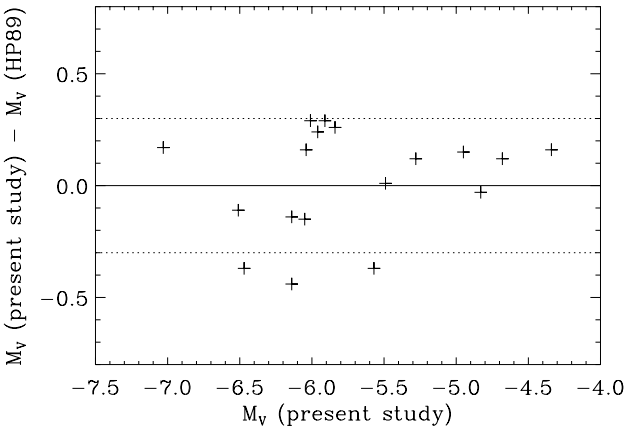

Fig. 1. Difference in absolute magnitude between our recalculations (using photometry by *Hipparcos*) and the values reproduced by Howarth & Prinja (1989), for those stars of our sample which belong to an association or cluster. The three outliers at the bottom correspond, from left to right, to HD 30 614, HD 209 975 and HD 36 861 (see text).

To avoid possible inconsistencies when adopting absolute magnitudes from different sources we recalculated the M_V of our targets using photometry and colours from *Hipparcos* (given in Cols. 4 and 5 of Table 1) combined with a mean intrinsic colour $(B-V)_0 = -0\overset{m}{.}31$ and $-0\overset{m}{.}28$ for stars of luminosity classes V/III and I, respectively (FitzGerald 1970; Wegner 1994) and an extinction law with $R = 3.1$, again, with the distances as mentioned above.

However, since the extinction can change significantly depending on the line of sight and since individual estimates of R for stars in several associations are available in the literature (Cardelli 1988; Clayton & Cardelli 1988; Cardelli et al. 1989), we decided to use these estimates as a second entry to determine absolute magnitudes. In particular, for objects in Cep OB2, in Per OB1 and in Ori OB1 the second entry for R is the average of more than one member.

As shown in Fig. 1, the obtained M_V values agree within $\pm 0\overset{m}{.}3$ with those published by Howarth & Prinja (1989) for all stars in common, except for HD 209 975, HD 36 861 and HD 30 614[1]. In the first two cases, the larger differences in M_V are due to relatively large differences between the *Hipparcos* photometry and the one used by Howarth & Prinja (1989). HD 30 614, on the other hand, is marked as a field star in Howarth & Prinja (1989) ($M_V = -6\overset{m}{.}0$), while in the present work we consider it as a member of the open cluster NGC 1502.

For several stars more than one entry is given in Table 1. This has been done to account for the "distance" problem inherent to *Galactic* objects mentioned in the introduction and to address the effects of using different radii on the resulting mass-loss and wind-momentum rates. The entry superscribed with number (1) accounts for the individual values of R as discussed above while the one superscribed with number (2) takes into account those stars which have been suggested by

[1] Note that with regard to absolute magnitudes the work of Howarth & Prinja (1989) is not a primary source, because the authors adopted these values from an unpublished catalogue by Garmany.

Table 1. Spectral types and photometric data of the studied stars. For objects with more than one entry, see footnote below and text.

Star HD	Spec. type	Assoc.	m_V mag	$B-V$ mag	R	d kpc	M_V mag
HD 190 429A	O4If+	CygOB3	6.62	0.148	3.1	2.29	−6.51
HD 66 811	O4I(n)f	Gum Nebula	2.21	−0.269	3.1	0.46	−6.14
HD 66 811[(2)]		field			3.1		−6.40*
HD 66 811[(4)]		runaway			3.1	0.73	−7.14
HD 16 691	O4If	PerOB1	8.69	0.411	3.1	2.29	−5.25
HD 16 691[(1)]		PerOB1			2.8	2.29	−5.04
HD 16 691[(3)]		runaway			3.1		−6.40*
HD 14 947	O5If$^+$	PerOB1	8.03	0.389	3.1	2.29	−5.84
HD 14 947[(1)]		PerOB1			2.8	2.29	−5.64
HD 14 947[(2)]		field			3.1		−6.90*
HD 210 839	O6I(n)f	CepOB2	5.05	0.192	3.1	0.83	−6.01
HD 210 839[(1)]		CepOB2			2.76	0.83	−5.85
HD 210 839[(2)]		runaway			3.1		−6.60*
HD 42 088	O6.5V	GemOB1	7.55	0.014	3.1	1.51	−4.35
HD 42 088[(5)]		GemOB1			3.1	2.00	−4.96
HD 54 662	O6.5V	CMaOB1	6.23	−0.018	3.1	1.32	−5.28
HD 192 639	O7Ib(f)	CygOB1	7.12	0.279	3.1	1.82	−5.91
HD 193 514	O7Ib(f)	CygOB1	7.42	0.392	3.1	1.82	−5.96
HD 34 656	O7II(f)	AurOB1	6.79	0.00	3.1	1.32	−4.68
HD 34 656[(6)]		AurOB2			3.1	3.02	−6.64
HD 47 839	O7V((f))	MonOB1	4.66	−0.233	3.1	0.71	−4.83
HD 24 912	O7.5I(n)((f))	PerOB2	3.98	0.016	3.1	0.40	−4.95
HD 24 912[(1)]		PerOB2	3.98		3.24	0.40	−4.99
HD 24 912[(2)]		runaway			3.1		−6.70*
HD 36 861	O8III((f))	OriOB1	3.39	−0.160	3.1	0.50	−5.57
HD 36 861[(1)]		OriOB1			5.0	0.50	−5.85
HD 210 809	O9Iab	CepOB1	7.56	0.010	3.1	3.47	−6.04
HD 207 198	O9Ib/II	CepOB2	5.94	0.312	3.1	0.83	−5.49
HD 207 198[(1)]		CepOB2			2.76	0.83	−5.29
HD 37 043	O9III	OriOB1	2.75	−0.210	3.1	0.50	−6.05
HD 37 043[(1)]		OriOB1			5.0	0.50	−6.24
HD 24 431	O9III	CamOB1	6.74	0.349	3.1	1.00	−5.30
HD 24 431[(1)]		CamOB1			3.51	1.00	−5.57
HD 16 429	O9.5I/II	CasOB6	7.70	0.530	3.1	2.19	−6.51
HD 30 614	O9.5Ia	NGC1502	4.26	−0.008	3.1	0.95	−6.47
HD 30 614[(2)]		runaway			3.1		−6.00*
HD 209 975	O9.5Ib	CepOB2	5.07	0.240	3.1	0.83	−6.14
HD 209 975[(1)]		CepOB2			2.76	0.83	−5.96
HD 18 409	O9.7Ibe	CasOB6	8.37	0.419	3.1	2.19	−5.50
HD 17 603	O7.5Ib(f)	field	8.49	0.551	3.1		−6.70*
HD 225 160	O8Ib(f)	field	8.19	0.260	3.1		−6.40*
HD 338 926	O8.5Ib(e?)	field	9.52	1.207	3.1		−6.60*
HD 188 209	O9.5Iab	field	5.60	−0.078	3.1		−6.00*
HD 202 124	O9.5Iab	field	7.74	0.209	3.1		−6.00*
HD 218 915	O9.5Iab	runaway	7.23	−0.026	3.1		−6.00*
BD +56 739	O9.5Ib	field	9.95	0.991	3.1		−6.00*
HD 47 432	O9.7Ib	field	6.23	0.086	3.1		−6.00*

*data corresponding to Garmany's spectral type–M_V calibration reproduced by Howarth & Prinja (1989).
(1) M_V computed with individual values for R (see text); (2) suggested to be a field/runaway star by Gies (1987); (3) suggested to be a runaway star by Stone (1979); (4) suggested to be a runaway star by Sahu & Blaauw (1993); (5) distance (as a member of NGC 2175 in GemOB1) given by Felli et al. (1977); (6) distance as a member of AurOB2 (Tovmassian et al. 1994).

Gies (1987) to be field or runaway stars, in contrast to the work by Humphreys (1978). In the latter case as well as for the stars listed in the lower part of Table 1 (i.e., field stars), absolute magnitudes derived with the same spectral type – M_V relation as used by Howarth & Prinja (1989) have been adopted. Entry number (3) relates to the work of Stone (1979) who suggested that HD 16 691 is a runaway star originating in the Galactic plane. Entry (4) refers to the work by Sahu & Blaauw (1993) who suggested, based on proper motion and radial velocity data, that the supergiant ζ Pup is a runaway star originating

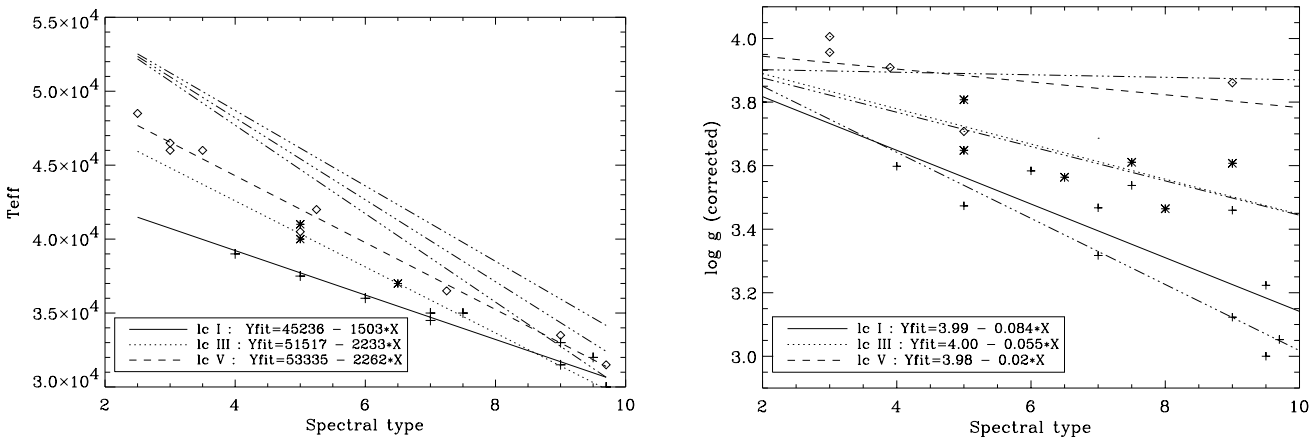

Fig. 2. Spectral type–$T_{\rm eff}$ (*left panel*) and spectral type–log g relations for luminosity class I (bold), III (dotted) and V (dashed) derived and used in the present study. Overplotted are the corresponding data from RPH and for lc V objects in the left panel also from Martins et al. (2002): crosses – lc I, asterisks – lc III, diamonds – lc V. The dotted-dashed lines represent the empirical calibrations obtained by Vacca et al. (1996) using data derived by means of pure H/He, non-LTE, plane-parallel, hydrostatic model atmospheres.

in the Vela Molecular Ridge close to the Vela R2 association. With a distance of 730 pc, ζ Pup would become the most luminous star in our sample. Entry (5) and (6) refer to comments given in Sect. 5.1.

4. Hα mass-loss rates

As noted in the introduction, one of the major goals of the present study is to check to what extent the analysis of Hα profiles alone can provide results consistent with those originating from a complete spectral analysis. To this end, we employed the approximate method developed by Puls et al. (1996) which we have modified to account for the effects of line-blocking and blanketing. This method uses H and HeII departure coefficients from unified model atmospheres parameterized in a simple way as a function of wind velocity together with photospheric NLTE line profiles as an inner boundary condition in order to obtain an "exact" (i.e., non-Sobolev) radiative transfer solution to synthesize the wind contaminated Hα-profile.

Detailed information about the actual fit procedure can be found in Puls et al. (1996). In the following, we will discuss how we obtain (i.e., approximate) those input parameters which are *not* varied throughout the fit, and how we account for line-blocking/blanketing effects.

4.1. Input parameters

Since we are going to use "only" Hα all stellar parameters including v_∞ have to be provided either from different sources or from calibrations.

Effective temperatures and surface gravities (Cols. 3 and 5 of Table 2) are determined from spectral types using own calibrations based on data obtained by RPH via line profile fitting to a number of strategic (hydrogen and helium) lines in the spectral range between 4000 and 6700 Å using NLTE atmosphere models with mass-loss, sphericity and an approximative treatment of metal line-blocking/blanketing.

Actually, not all of the stars studied by RPH have been included to derive the spectral type – $T_{\rm eff}$ relation: close binaries (HD 93 129A and HD 303 308, Nelan et al. 2003) as well as fast rotators (e.g., HD 217 086 with $v \sin i$ = 350 km s^{-1} and HD 13 268 with $v \sin i$ = 300 km s^{-1}) were excluded. The former due to a possible influence of the secondary on the "observed" temperatures and the latter because of the effects of stellar rotation on the surface temperature distribution (gravity darkening).

Since there was only a small number of luminosity class V stars left after the reduction of the Repolust sample we incorporated data presented by Martins et al. (2002) in a comparable investigation. (With respect to $\log g$, we used the Repolust sample alone.) Figure 2 shows the temperature (left panel) and $\log g$ (right panel) calibrations for luminosity classes I, III and V derived and used in the present study.

One can see that the scatter of the $T_{\rm eff}$ data around the regression lines is relatively small (σ = 950, 360 and 793 K, for lc I, III and V, respectively), while in the case of the spectral type–$\log g$ relations it is somewhat larger (σ = 0.12, 0.17 and 0.20). On the other hand, the reader may note that the $T_{\rm eff}$ calibration for late spectral types (later than O7) remains somewhat uncertain due to the strong influence of the specific wind-density on $T_{\rm eff}$. The dotted-dashed lines overplotted in each panel represent the empirical calibrations obtained by Vacca et al. (1996) using data derived by means of pure H/He, non-LTE, plane-parallel, hydrostatic model atmospheres.

Our results indicate that the differences between the blanketed and the unblanketed temperature scale decrease with decreasing $T_{\rm eff}$, being largest (max($\Delta T_{\rm eff}$) $\sim$ 10 000 K) for luminosity class I and smallest (max($\Delta T_{\rm eff}$) $\sim$ 5000 K) for luminosity class V stars due to the additional wind blanketing present in supergiant atmospheres.

On the other hand, the $\log g$ regressions for luminosity classes III and V based on blanketed models are almost identical to the calibration by Vacca et al., while for (late) supergiants an increase of less than 0.15 dex is found, in agreement with

Table 2. Stellar and wind parameters of the O-star sample, derived from calibrations discussed in Sect 4.1 and by Hα line fitting. Stars with more than one entry correspond to the entries in Table 1 and differ mainly in the adopted stellar radius and in the dependent quantities. Spectral types abbreviated, cf. Table 1. Bold face numbers for $\log L$ and $D_{\rm mom}$ indicate the preferred solution that is used in our final analysis of the WLR ("case C", cf. Sect. 5.1) while italics for β mark values *derived* from emission type profiles. Modifications of departure coefficients for HeII given as *multipliers* $r_{4,6}$ to standard values from Puls et al. (1996). Modifications of departure coefficients for hydrogen are given by absolute numbers, $b_2^{\rm in}/b_3^{\rm in}$. "pt" indicates whether Hα is in absorption or emission. Luminosity L in $L_\odot$, $v \sin i$ and v_∞ in units of km s^{-1}, $\dot{M}$ in 10^{-6} $M_\odot$/yr, modified wind-momentum rate $D_{\rm mom} = \dot{M} v_\infty (R_\star/R_\odot)^{0.5}$ in cgs and $Q = \dot{M}/(R_\star/R_\odot)^{1.5}$ in units of $M_\odot$/yr.

Object	Sp	$M_{\rm V}$	$T_{\rm eff}$	$R_\star$	$\log g$	$Y_{\rm He}$	$v \sin i$	$\log L$	v_∞	$\dot{M}$	β	$r_4^{\rm in}/r_6^\infty$	$b_2^{\rm in}/b_3^{\rm in}$	$\log D_{\rm m}$	$\log Q$	pt
HD 190 429A	O4I	−6.51	39 200	20.8	3.65	0.14	135	**5.97**	2 400	14.2	*0.95*	1.05/		**29.99**	−6.82	e
HD 66 811	O4I	−6.14	39 200	17.5	3.65	0.20	203	**5.82**	2 300	6.4	*0.92*		/1.05	**29.59**	−7.06	e
HD 66 811(2)		−6.40		19.8				5.92		7.6			/1.05	29.69	−7.06	
HD 66 811(4)		−7.14		27.8				**6.22**		12.8			/1.05	**29.99**	−7.06	
HD 16 691	O4I	−5.25	39 200	11.6	3.65	0.10	140	5.46	2 300	5.6	*0.96*			29.46	−6.85	e
HD 16 691(1)		−5.04		10.6				5.38		4.9				29.38	−6.85	
HD 16 691(3)		−6.40		19.8				**5.92**		12.5				**29.92**	−6.85	
HD 14 947	O5I	−5.84	37 700	15.7	3.56	0.20	133	5.65	2 300	7.7	*0.98*	1.15/	/1.45	29.65	−6.91	e
HD 14 947(1)		−5.64		14.3				5.57		6.67		1.15/	/1.45	29.56	−6.91	
HD 14 947(2)		−6.90		25.6				**6.08**		16.0		1.15/	/1.45	**30.07**	−6.91	
HD 210 839	O6I	−6.01	36 200	17.5	3.48	0.10	214	5.68	2 200	5.1	*1.00*	1.05/	2./	29.47	−7.16	e
HD 210 839(1)		−5.85		16.3				5.62		4.6		1.05/	2./	29.41	−7.16	
HD 210 839(2)		−6.60		23.0				**5.91**		7.7		1.05/	2./	**29.71**	−7.16	
HD 42 088	O6.5V	−4.35	38 600	7.7	3.85	0.12	62	5.08	2 200	0.38	0.85	1.3/		28.17	−7.75	a
HD 42 088(5)		−4.96		10.7				**5.36**		0.62		1.3/		**28.45**	−7.75	
HD 54 662	O6.5V	−5.28	38 600	11.9	3.85	0.12	85	**5.45**	2 450	0.6	0.80			**28.50**	−7.84	a
HD 192 639	O7Ib	−5.91	34 700	17.2	3.39	0.20	110	**5.59**	2 150	5.3	*1.09*	1.25/.80		**29.47**	−7.13	e
HD 193 514	O7Ib	−5.96	34 700	17.6	3.39	0.10	95	**5.61**	2 200	2.7	0.80		/1.48	**29.20**	−7.44	a
HD 34 656	O7II	−4.68	34 700	9.8	3.50	0.12	85	5.10	2 150	0.62	1.09	1.5/		28.42	−7.69	a
HD 34 656(6)		−6.64		24.1				**5.88**		2.40		1.5/		**29.20**	−7.69	
HD 47 839	O7V	−4.83	37 500	9.9	3.84	0.10	62	**5.24**	2 200	1.2	0.75			**28.72**	−7.41	a
HD 24 912	O7.5I	−4.95	34 000	11.2	3.35	0.15	204	5.18	2 400	1.19	0.78	1.3/.85		28.78	−7.50	a
HD 24 912(1)		−4.99		11.5				5.20		1.23		1.3/.85		28.80	−7.50	
HD 24 912(2)		−6.70		25.2				**5.88**		4.0		1.3/.85		**29.48**	−7.50	
HD 36 861	O8III	−5.57	33 600	15.1	3.56	0.10	66	5.42	2 400	0.8	0.80			28.67	−7.87	a
HD 36 861(1)		−5.85		17.2				**5.53**		0.97				**28.78**	−7.87	
HD 210 809	O9Iab	−6.04	31 700	19.6	3.23	0.14	100	**5.54**	2 100	4.5	*0.91*	1.1/		**29.42**	−7.29	e
HD 207 198	O9Ib/II	−5.49	31 700	15.2	3.23	0.12	85	5.32	2 100	0.9	0.97	1.3/		28.67	−7.82	a
HD 207 198(1)		−5.29		13.9				**5.25**		0.79		1.3/		**28.59**	−7.82	
HD 37 043	O9III	−6.05	31 400	19.8	3.50	0.12	120	5.54	2 300	1.2	0.85	1.6/		28.89	−7.87	a
HD 37 043(1)		−6.24		21.6				**5.61**		1.37		1.6/		**28.97**	−7.86	
HD 24 431	O9III	−5.30	31 400	14.0	3.50	0.12	90	5.24	2 150	0.3	0.95	1.3/		28.18	−8.24	a
HD 24 431(1)		−5.57		15.9				**5.35**		0.36		1.3/		**28.29**	−8.25	
HD 16 429	O9.5I/II	−6.51	31 000	24.8	3.19	0.10	80	**5.71**	1 600	1.4	0.85	1.3/.9		**28.85**	−7.95	a
HD 30 614	O9.5Ia	−6.47	31 000	24.9	3.19	0.10	100	5.71	1 550	4.2	*1.05*	1.3/		29.31	−7.47	e
HD 30 614(2)		−6.00		19.6				**5.51**		2.9		1.3/		**29.10**	−7.48	
HD 209 975	O9.5Ib	−6.14	31 000	20.9	3.19	0.10	90	5.56	2 050	1.8	0.80	1.3/	/1.42	29.03	−7.72	a
HD 209 975(1)		−5.96		19.2				**5.49**		1.58		1.3/	/1.42	**28.95**	−7.73	
HD 18 409	O9.7Ib	−5.50	30 600	15.7	3.17	0.14	110	**5.29**	1 750	1.5	0.70			**28.82**	−7.62	a
HD 17 603	O7.5Ib	−6.70	34 000	25.2	3.35	0.12	110	5.88	1 900	5.90	*1.05*	1.1/		29.55	−7.33	e
HD 225 160	O8Ib	−6.40	33 000	22.4	3.31	0.12	125	5.73	1 600	5.3	*0.85*	1.5/.9		29.40	−7.30	e
HD 338 926	O8.5Ib	−6.60	32 500	22.7	3.27	0.12	80	5.72	2 000	5.7	*1.00*			29.53	−7.28	e
HD 188 209	O9.5Iab	−6.00	31 000	19.6	3.19	0.12	87	5.51	1 650	1.6	0.90	1.4/	/1.47	28.87	−7.73	a
HD 202 124	O9.5Iab	−6.00	31 000	19.6	3.19	0.12	140	5.51	1 700	3.2	*1.25*	1.4/.7		29.18	−7.43	e
HD 218 915	O9.5Iab	−6.00	31 000	19.6	3.19	0.12	80	5.51	2 000	1.7	0.95	1.2/	/1.54	28.98	−7.71	a
BD+56 739	O9.5Ib	−6.00	31 000	19.6	3.19	0.12	80	5.51	2 000	2.3	0.85	1.35/	/1.33	29.02	−7.61	a
HD 47 432	O9.7Ib	−6.00	30 500	18.9	3.17	0.12	95	5.45	1 600	1.9	*1.03*	1.4/.8	/1.07	28.92	−7.64	e

what might be expected from theory (different density stratification in hydrostatic vs. mass-losing atmospheres in those regions where the Balmer line wings are formed, cf. Puls et al. 1996). All gravities displayed in Fig. 2 have been corrected for the effects of centrifugal forces (similarly to the procedure applied by Herrero et al. 1992; Vacca et al. 1996 and particularly RPH), since many of the stars from the Repolust sample have projected rotational speeds exceeding of 200 km s^{-1}. For the faster rotators in our sample, we have finally re-corrected the derived $\log g$ values in order to use photospheric input profiles with appropriate *effective* gravities in our Hα line-profile fitting procedure.

We are aware of the fact that the spectral type – $T_{\rm eff}$ relationship may not be linear, e.g. Crowther (1998). Note, however, that the data used here do not give any evidence of significant deviations from a linear approximation, at least not in the covered range of spectral subclasses. In particular, using a cubic, instead of a linear regression for stars with stronger (lc I) and weaker (lc V) winds improves the fit quality by less than 100 K, which is much smaller than the typical error in $T_{\rm eff}$ ($\pm$1000...1500 K) derived from complete spectral analyses (e.g., Herrero et al. 1992; RPH). Admittedly, our calibration might be somewhat unrealistic for the earliest spectral types at luminosity class III. Note, however, that our sample does not comprise any objects in this range, and therefore our analysis is not affected by this uncertainty.

Stellar radii (Col. 4 of Table 2) have been derived from dereddened absolute magnitudes and theoretical fluxes in the V-band using the procedure outlined by Kudritzki (1980), cf. Eqs. (1) and (2) in RPH. The theoretical fluxes have been approximated by using a radiation temperature of $T_{\rm rad} \approx 0.9\ T_{\rm eff}$ (V-band!), where this approximation results from an analysis of line-blanketed O-star model atmospheres. The typical accuracy of this approximation (which translates almost linearly into the derived radii) is of the order of 5% in the O-star domain.

Helium abundance. For those stars in common with the sample by Repolust et al. we have adopted their helium abundance. For the remainder, we have used a "normal" abundance of $Y_{\rm He} = N({\rm He})/N({\rm H}) = 0.1$ as a first guess. Subsequently, this value was increased, if necessary, to obtain a better fit (with respect to the HeII blend), accounting also for the evolutionary phase (dwarf/supergiant) of the objects. Therefore, these values can be considered only as rough estimates.

Radial and rotational velocities. Puls et al. (1996) noted that the accuracy of the adopted radial velocity, $v_{\rm r}$, should be better than 20 km s^{-1} in order to obtain reliable fit results. In the present study, radial velocities (not listed in Table 2) and projected rotational velocities $v \sin i$ (Col. 7 of Table 2) of the sample stars hotter than 35 500 K are taken from the General Catalogue of Mean Radial Velocity (GCMRV, Barbier-Brossat & Figon 2000) and from Penny (1996), respectively, except for HD 16 691, for which we have used our own estimate of $v \sin i$ (see below).

For stars cooler than 35 500 K, with the exception of HD 36 861, HD 338 926 and HD 188 209, we obtained own estimates for $v \sin i$ and $v_{\rm r}$ by means of fitting the HeI λ6678 absorption line. The reliability of our determinations has been checked by comparison with data from other investigations. In particular, our set of $v \sin i$ estimates conforms quite well (within $\pm$10 km s^{-1}) with those from Penny (1996) for 9 out of 11 objects in common. In the exceptional cases of HD 36 861 and HD 188 209 our estimates of $v \sin i$ turned out to be larger (by $\sim$30%) than those from Penny, and the estimates of Penny have been adopted.

Good agreement was also found between our set of $v_{\rm r}$ data and that of Conti et al. (1977) (within $\pm$20 km s^{-1}) for 13 stars in common. The Hα spectrum of HD 338 926 does not include HeI λ6678. Hence, no estimates of either $v \sin i$ or $v_{\rm r}$ could be derived. We adopted $v_{\rm r}$ from the SIMBAD Catalogue and a typical value of 80 km s^{-1} for $v \sin i$.

Wind terminal velocities (Col. 9 of Table 2) have been derived by interpolating various estimates available in the literature (Haser 1995; Howarth et al. 1997; Lamers et al. 1995; Groenewegen et al. 1989), except for HD 16 691, HD 225160, HD 17 603, HD 338926, BD+56 739 and HD 18 409. For the first two of the latter stars we derived a v_∞ – estimated by means of line-profile fitting of UV lines available from the INES IUE archive (`http://ines.hia.nrc.ca/ines`), while for the remaining four objects we used the calibration provided by Kudritzki & Puls (2000).

Radiation temperatures at Hα and photospheric profiles. To account for the effects of line blanketing, we have used a value of $T_{\rm rad} = 0.91\ T_{\rm eff}$ for luminosity class I objects and $T_{\rm rad} = 0.86\ T_{\rm eff}$ for the other luminosity classes, where these values originate from a calibration of a large grid of (line-blanketed) model fluxes calculated by Puls et al. Note that for unblanketed model atmospheres this value is much lower, i.e., of the order of $0.77\ T_{\rm eff}$ (cf. Puls et al. 1996).

In principle, the photospheric input profiles have to be recalculated as well. Because of the insensitivity of the Balmer lines to changes in $T_{\rm eff}$ *in the O-star domain* (differences up to 5000 K result only in marginal changes), however, we employed the same (unblanketed) grid of line profiles as described in Puls et al. (1996), evaluated at the "new" effective temperatures, of course.

The only quantities left to be specified are the wind minimum velocity $v_{\rm min}$ and the electron temperature $T_{\rm e}$. Following Puls et al., we adopt $v_{\rm min} = 1$ km s^{-1} and $T_{\rm e} = 0.75\ T_{\rm eff}$, which are the values consistent with the parameterized run of the H/He departure coefficients. A comparison with Hα profiles from the consistent analysis performed by RPH convinced ourselves finally that this parameterization remains roughly unaffected by blanketing effects, at least if the values of $T_{\rm rad}$ as cited above were used.

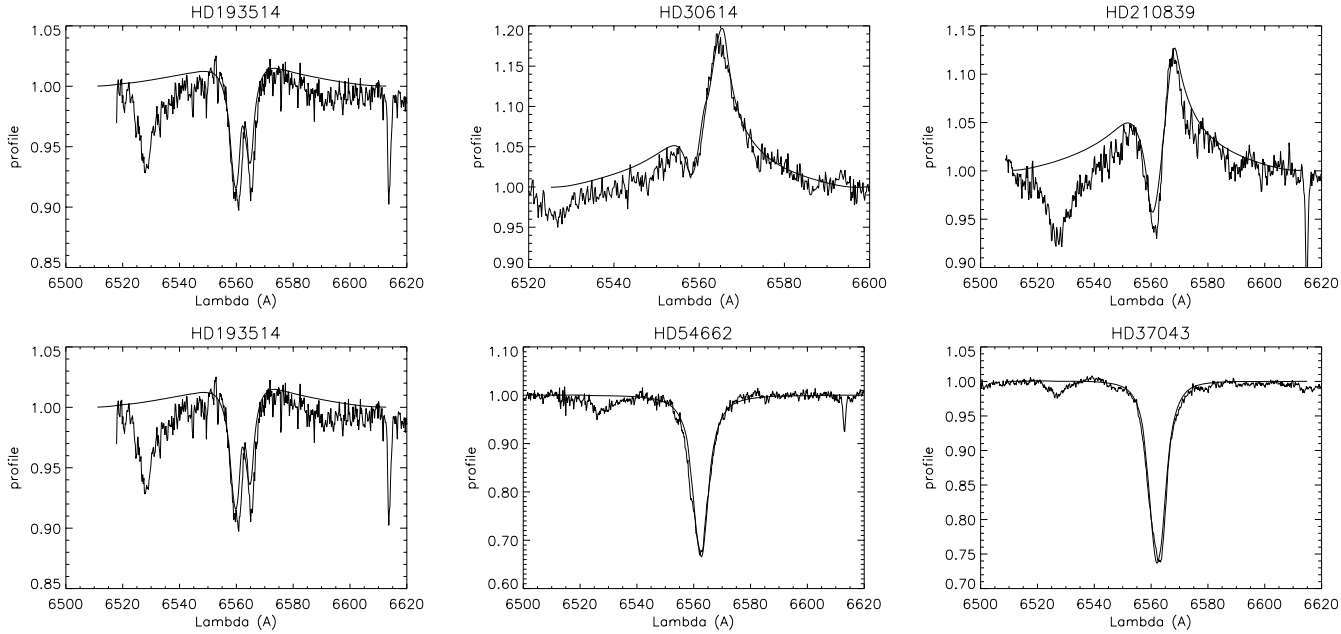

Fig. 3. Examples of differently shaped Hα profiles from stars of our sample together with the corresponding model fits.

4.2. Results

4.2.1. General remarks

When performing the individual profile fits, it turned out that most of the supergiants exhibit Hα profiles with a blue wing that cannot be well reproduced with the adopted "standard" parameterization of the HeII departure coefficients. To fit these profiles, we were forced to increase the He-opacity in the inner wind part – corresponding to an increase in the departure coefficient $b_4^{\rm in}$ typically by a factor $r_4^{\rm in} = 1.3$ – and, in a few cases, to reduce the emissivity outside, i.e., to lower b_6^{∞} (a typical factor here is $r_6^{\infty} \approx 0.8$). The same problem was noted by Puls et al. (1996) who attributed this to the neglect of the effects of (EUV) line blocking which become particularly important in dense winds. Our results indicate a similar trend (remember, that we use the "standard" parameterization derived from unblocked models) with a somewhat smaller correction though compared to the results by Puls et al., which most probably is due to the increased ratio of $T_{\rm rad}$ / $T_{\rm eff}$ in our modified approach.

Concerning the run of the hydrogen departure coefficients, we found that the adopted "standard" parameterization does not pose any problems when used to fit the lines of the observed profiles. In general, an almost perfect fit to any kind of profile (emission, absorption, P Cygni type) was obtained.

The only problems we have found so far are related to the following profile types in supergiants:

i) profiles exhibiting a strong decline from the emission maximum towards the absorption minimum, e.g., from HD 66 811, HD 14 947 and HD 47 432;
ii) profiles showing Hα in absorption with a central emission, e.g., from HD 193 514, HD 209 975, HD 188 209, HD 218 915 and BD+56 739.

To fit these profiles, in all but two of the above cases we were forced to enhance the Hα emissivity, i.e., to increase $b_3^{\rm in}$ (typically, from the "standard" value 1.2 to a value of 1.4). For HD 66 811 and HD 47 432, the Hα emissivity in the inner wind part had to be reduced (typically, $b_3^{\rm in} \approx 1.05$). Finally, in the case of HD 210 839, we had to increase the Hα opacity in the inner wind part. Let us point out that all these modifications are more or less "cosmetic", i.e., they lead "only" to an optically almost perfect fit. The decisive parameters obtained from the fit, however, $\dot{M}$ and β (see below), remain at the same value as if one uses the "standard" parameterization. Typical examples of differently shaped profiles together with the corresponding model fits are shown in Fig. 3.

As noted by Puls et al. (1996), objects with Hα in emission allow to derive the velocity parameter β in parallel with the mass-loss rate. For these objects (with β given as italic numbers in Table 2), we find an average value of $\beta = 1.02 \pm 0.09$. For objects with Hα in absorption, we used $\beta = 0.8$ (expected from theory for thin winds) as a starting value and improved this value from the line fit, where possible. In these cases, of course, the uncertainty in β and, thus, in $\dot{M}$ (cf. Kudritzki & Puls 2000; Puls et al. 1996) is much larger than in the cases where β can be derived unambiguously (at least with respect to the "standard model" of winds) and will, therefore, be considered separately in our error analysis.

It is worth noting that for ζ Pup – for which a fit using unblanketed models resulted in $\beta = 1.15$ (Puls et al. 1996) – we find $\beta = 0.92$, in agreement with the recent optical analysis by RPH, and much closer to the results from UV line-profile fits, $\beta_{\rm UV} = 0.7 \ldots 0.8$, see Groenewegen & Lamers (1989) and Haser (1995).

For one star in our sample, HD 202 124, we have obtained a rather large value, $\beta = 1.25$. This object is a supergiant of spectral type O9.5 which shows, in contrast to the other supergiants of the same spectral type in our sample, a P Cygni-like profile with an absorption dip that seems too strong to be solely due to absorption from the HeII blend. In particular, this

absorption feature cannot be fitted by simply "playing" with the H/He departure coefficients.

Finally, we like to point out that the last two plots of Fig. 3 allow to assess the quality of our $\log g$ calibration (Sect. 4.1). Since we did *not* vary the gravity during our fit procedure but always used the value derived by means of our calibration, the almost perfect agreement between observed and modeled line wings indicates a rather high precision of this calibration.

4.2.2. Error analysis

In the following, we briefly describe our error analysis which will become important in the next section when deriving the wind-momentum luminosity relation for our sample.

In order to assess the errors in $\log L$ and $\log D_{\rm mom}$ we followed the philosophy outlined in detail by RPH. To estimate the uncertainty in the stellar radius, we applied their Eq. (8) with $\Delta M_{\rm V} = \pm 0.3$ and $\Delta T_{\rm eff} = \pm 1500$ K. The former value is in accordance with the results displayed in our Fig. 1, while the latter reflects the uncertainties in our spectral type – $T_{\rm eff}$ calibration and in the underlying data base, cf. Fig. 2. With these estimates, the error in the stellar radius is dominated by the uncertainty in $M_{\rm V}$ and is of the order of $\Delta \log R_\star \approx \pm 0.06$, i.e., roughly 15%.

Specified in this way, the error in luminosity is given by

$$\Delta \log L \approx \sqrt{(4\,\Delta \log T_{\rm eff})^2 + (2\,\Delta \log R_\star)^2} \qquad (1)$$

and results in $\Delta \log L \approx \pm 0.15$, i.e., the error due to $\Delta R_\star$ is somewhat larger than due to $\Delta T_{\rm eff}$.

To assess the errors in the wind-momentum rate, let us first analyze the errors in $\dot{M}$ inherent to our analysis. Actually, any line-fit to Hα does not specify $\dot{M}$ itself, but only the quantity Q introduced by Puls et al. (1996),

$$Q = \frac{\dot{M}}{R_\star^{1.5}}. \qquad (2)$$

In particular, any change in $R_\star$ leads to an identical fit if $\dot{M}$ is adapted in such a way that Q remains constant (compare Table 2 for those objects with more than one entry). Thus, Q is the quantity for which the error has to be evaluated.

For emission profiles, where also β can be constrained from the fit, we estimate the precision of the derived Q as ±20% (from the fit quality). For absorption profiles, we have varied β typically by ±0.1 (or more, if necessary), and obtained the corresponding upper and lower boundaries of $\dot{M}$ (actually, of Q) from additional fits to the observed profiles. The results of this procedure are displayed in Table 3. When these error estimates were smaller than the adopted error from above (i.e., ±20%), the latter value was chosen as a conservative minimum. Note that the maximum errors in Q can reach factors of almost two (for absorption profiles)!

From the error in Q, the uncertainty in the derived wind-momentum rate, $D_{\rm mom} = Q v_\infty R_\star^2$, can be calculated via

$$\Delta \log D_{\rm mom} \approx \sqrt{(\Delta \log Q)^2 + (2\,\Delta \log R_\star)^2 + (\Delta \log v_\infty)^2}\,. \qquad (3)$$

Note that the error in $R_\star$ enters again quadratically. The errors in v_∞ have been assumed to be ±150 km s^{-1} or larger, if either the different sources for v_∞ do not coincide or v_∞ has been obtained from calibrations. Thus, in most cases the resulting error in $\log D_{\rm mom}$ is of the order of ±0.15, i.e., similar to the error in $\log L$.

Table 3. Objects with Hα in absorption: variation in derived $\dot{M}$, if β is modified within the typical uncertainties, $\beta^- < \beta < \beta^+$, with $\Delta\beta$ of order 0.1. $\dot{M}$ in units of 10^{-6} $M_\odot$/yr.

Object	β	$\dot{M}$	β^-	$\dot{M}^+$	β^+	$\dot{M}^-$
HD 42088	0.85	0.38	0.75	0.46	0.95	0.30
HD 54662	0.80	0.60	0.70	0.90	0.90	0.40
HD 193514	0.80	2.70	0.70	3.24	0.90	2.05
HD 34656	1.09	0.62	0.80	0.95	1.20	0.50
HD 47839	0.75	1.20	0.65	1.50	0.90	0.95
HD 24912[(2)]	0.78	4.00	0.65	5.00	0.90	3.00
HD 36861	0.80	0.80	0.70	1.40	0.90	0.64
HD 207198	0.97	0.90	0.80	1.25	1.10	0.70
HD 37043	0.85	1.20	0.75	1.50	0.95	0.96
HD 24431	0.95	0.30	0.80	0.60	1.05	0.24
HD 16429	0.85	1.40	0.75	1.70	0.95	1.12
HD 209975	0.80	1.80	0.70	2.16	0.90	1.44
HD 18409	0.70	1.50	0.65	1.80	0.90	0.90
HD 188209	0.90	1.60	0.80	1.92	1.00	1.28
HD 218915	0.95	1.70	0.80	2.04	1.05	1.30
BD+56739	0.80	2.15	0.70	2.58	0.90	1.72

4.3. Comparison with results from a complete analysis

The basic outcome of our approximate analysis, namely the Q-value, is listed in Table 2. Before we discuss further consequences and as outlined in the introduction, we have to convince ourselves that the estimates derived for this quantity are consistent with the results of the complete analysis. That way, we particularly verify our modifications concerning the effects of line-blocking/blanketing.

Any Q-value derived from Hα profiles should be almost independent of stellar parameters if in the underlying models the same terminal velocities were used and if the influence of different effective temperatures were considered by applying the temperature correction given in Puls et al. (their Eqs. (48) and (49)). In our comparison with the Repolust sample for 11 stars in common (Fig. 4) we have performed such a correction.

This figure shows that at higher values of $\log Q$, i.e., denser winds, the agreement is excellent (within 0.06 dex). On the other hand, at lower values the differences can become significant, e.g., for HD 207 198, HD 18 409 and HD 24 912. From Table 2, last column, we see that the Hα profiles of these stars all appear in absorption. Insofar, the above mentioned β-problem might be a reason of this discrepancy, and a closer inspection of the corresponding errors (see Table 3) reveals that this actually is the major source of disagreement.

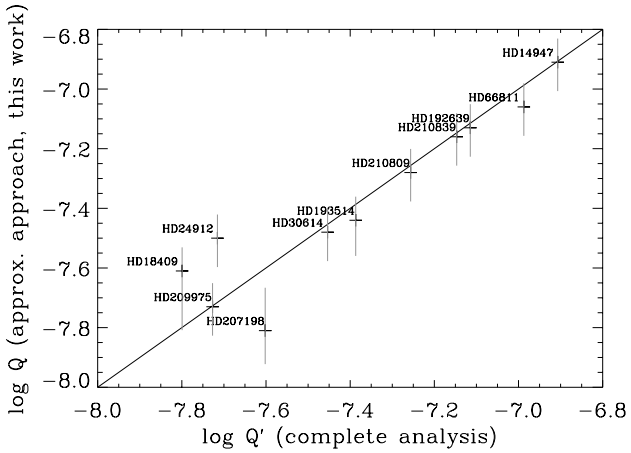

Fig. 4. Comparison of derived Q-values from our analysis with corresponding data from RPH, for eleven stars in common. The Q-values of the complete analysis have been corrected for differences in effective temperature. Overplotted are the individual error bars calculated according to Sect. 4.2.2. For a discussion concerning the outliers, see text.

The remaining disagreement of <0.1 dex (in those cases where the formal errors are still too low) more likely reflects real variability in the strength of the studied winds. Note, e.g., that mass-loss variations of up to ~45% have been suggested by Markova & Scuderi (2003) to explain the variability of the Hα emissivity observed in our sample stars over a 2 yr period. Interpreted in this way, the disagreement found here would indicate variations of the same order. A comparison of our Hα profiles with those analysed by Repolust et al. for the three stars with largest differences in log Q showed that for each star the corresponding profiles differ in the correct sense.

Finally, let us explicitly state that the discrepancy found at low wind densities is *not* related to the problems we have partly met when fitting Hα profiles in absorption, (i.e., to the required modifications of departure coefficients), since the final values of $\dot{M}$ are only weakly affected by this procedure: the line opacity scales with $\dot{M}^2$ but only linearly with the b_i's.

5. Wind-momentum rates and WLR

Table 2 summarizes all stellar and wind parameters derived (and adopted) for our sample stars as described in the previous section. Before we proceed towards an analyis of the corresponding WLR, let us give some

Remarks on individual objects. A closer inspection of the available data reveals that at least in three cases, HD 16 619, HD 24 912 and HD 34 656, the derived values for M_V , and accordingly $R_\star$, seem to be inconsistent with the adopted spectral type/luminosity class and the available spectroscopy. The estimates of $R_\star$ for HD 16 619 (as a member of the Double Cluster χ and ξ Persei), derived with the standard and the individual extinction ratio are both a factor of two lower than the radii of the other two sample stars of same spectral type.

The reason for this discrepancy is most likely related to the fact that the distance to this star is very uncertain (Stone 1979; Walborn 2002). Thus, in the following we will preferentially use the parameters resulting from a calibration of M_V, i.e., entry (3).

The second star with dubious parameters is HD 24 912. If one follows the plausible arguments given by Herrero et al. (1992) that this star is a supergiant, then its radius cannot be of the order of 11 $R_\odot$. On the other hand, if one believes that it is a normal giant, then its wind-momentum is too high for a luminosity class III object. The situation does not improve if the individual extinction ratio is adopted. The possibility that HD 24 912 is not a member of PerOB2 but a runaway star (Gies 1987) seems to resolve the problem, and also for this star we will use the parameters resulting from a calibration of M_V (entry (2)).

Humphreys (1978) has listed HD 34 656 as a member of Aur OB1 (d = 1.32 kps). However, the $R_\star$ derived when adopting this distance is rather low, a factor of two lower than the radii of the other two supergiants of same spectral type. On the other hand, Tovmassian et al. (1994) argue that HD 34 656 is a member of a small group of stars located at the distance of AurOB2 (d = 3 kpc). Although the values for M_V and $R_\star$ resulting from this distance seem a bit too large for the adopted spectral type/luminosity class, we will use these parameters (entry (6)) until further evidence, cf. Sect 5.1.

Two other objects deserve special attention as well. HD 42 088 is listed as a member of GemOB1 (d = 1.5 kpc) by Humphreys (1978). However, Felli et al. (1977) identified this object as a member of NGC 2175 for which several independent distance determinations exist, ranging from 1.91 to 2.87 kpc. Thus, a distance of 2 kpc as adopted by Felli et al. (1977) seems to be a good compromise for HD 42 088, also with respect to its radius, and we will use this value in the following (entry (5)).

For ζ Pup (HD 66 811), the values resulting from both its "conventional" distance of 460 pc and a calibration of M_V (entry (2)) overlap within the adopted errors, and we will preferentially use the "standard" values for this star. In addition, we will follow the suggestion by Sahu & Blaauw (1993) that this star is a runaway star originating from the Vela Molecular Ridge and has a distance of 730 pc. With this value and adopting a standard reddening, the radius of ζ Pup becomes 28 $R_\odot$ which is rather large for its spectral type. Interestingly, a present investigation by Pauldrach et al. (in prep. for A&A) seems to favour such a large value in terms of both a self-consistent hydrodynamical wind model and the corresponding synthetical UV spectrum, when compared to observations. In what follows we will use this entry (4) as a second choice in order to consider its possible relevance within the wind-momentum luminosity relation.

Hereafter, we will denote HD 16 691, HD 24 912, HD 34 656 and HD 42 088 as "peculiar objects".

5.1. WLR as function of luminosity class

From now on, we will concentrate on the second major objective of the present investigation, namely on the wind-momentum luminosity relation (WLR) for Galactic O-type

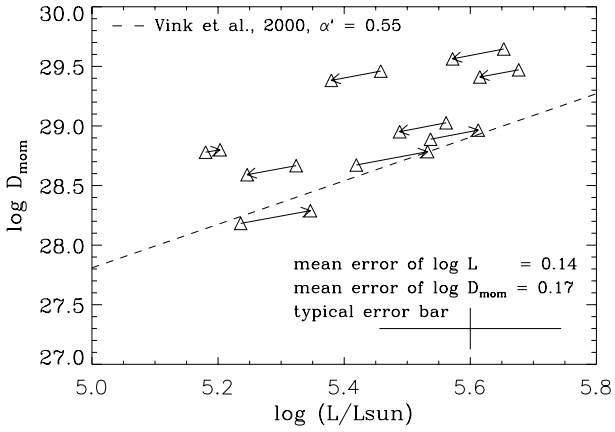

Fig. 5. Influence of uncertainty in reddening on modified wind-momenta and luminosities. Arrows point from positions resulting from standard reddening, $R = 3.1$, to positions resulting from adopting individual values for R (entries with superscript (1) in Tables 1 and 2). Dashed: theoretical WLR predicted by Vink et al. (2000).

stars. We begin with considering the consequences of "fine tuning" direct and indirect parameters entering the WLR.

Let us first comment on the influence of using different values for the total to selective extinction, R. The larger R, the brighter the star is in the visual, and the larger the stellar radius. Since we are fitting for Q, also the mass-loss and the wind-momentum rate increases, as well as the (bolometric) luminosity. Even in cases of an "extreme" extinction ratio of 5.0, however, the resulting differences in $R_\star$ and $\dot{M}$ are small, roughly 10–14% of the values derived with $R = 3.1$. (Hereafter all data obtained using $R = 3.1$ will be referred to as "standard" values). The corresponding variations in $\log L$ and $D_{\rm mom}$ are 0.11 dex and 0.08 dex, respectively, as shown in Fig. 5, and are (much) smaller than the individual uncertainties for these quantities. Moreover, the corresponding shifts are almost in parallel to any expected wind-momentum luminosity relationship (for comparison, we have overplotted the theoretical relation provided by Vink et al. 2000), so that any uncertainty in R should by of minor influence on the results discussed below.

In addition to the effect caused by using different redding laws, there is also the distance problem, which, taken together, forced us to deal with more than one entry for many of our sample objects (cf. Sect. 3). Consequently, various combinations have to be accounted for, and we decided to consider the following different cases (A to C without field stars):

- Case A includes those entries without any superscript (standard, i.e., (almost) all distances from Humphreys (1978) and $R = 3.1$) plus the specific values adopted for "peculiar objects" as discussed above.
- Case B refers to entries with superscript 1 (individual reddening) plus "peculiar objects" + data without superscript for the rest of the stars.
- Case C combines data with superscript 2 plus "peculiar objects" plus data with superscript 1 (if no entry with superscript 2 available) plus standard values for the rest.
- Case D comprises case C plus field stars.

In Fig. 6 we have displayed the WLRs based on the datasets corresponding to case A, which is the starting point of our investigation, and case D, which is the ending point. Numbers correspond to luminosity classes.

Linear regressions, obtained by means of χ^2 minimization accounting for the individual errors (calculated as described in Sect. 4.2.2) in *both* directions, are shown as solid (l.c. I/II) and dotted (l.c. III/V) lines. We have used the conventional formulation

$$\log D_{\rm mom} = x \log(L/L_\odot) + D_{\rm o} \tag{4}$$

with exponent x being the inverse of α', which corresponds to the slope of the line-strength distribution function corrected for ionization effects (Puls et al. 2000; Kudritzki & Puls 2000).

To our knowledge, this investigation together with that of RPH are the first to account for errors in both directions. Our approach follows the principal arguments given by Press et al. (1992, Sect. 15.3, and references therein), i.e., the parameters of the regression follow from minimizing

$$\chi^2(x, D_0) = \sum_i \frac{(\log D_{{\rm mom},i} - x \log L_i/L_\odot - D_{\rm o})^2}{{\rm Var}_{{\rm tot},i}} \tag{5}$$

with *total* variance $\rm Var_{tot}$,

$${\rm Var}_{{\rm tot},i} = {\rm Var}\,(\log D_{{\rm mom},i} - x \log L_i/L_\odot - D_{\rm o}). \tag{6}$$

Since $\log D_{\rm mom}$ and $\log L$ are statistically dependent (via $R_\star^2$, a case not considered by Press et al.), one has to account for the covariance between both terms. Thus, we have

$$\begin{aligned} {\rm Var}_{{\rm tot},i} \;=\; & {\rm Var}\,(\log D_{{\rm mom},i}) + x^2\,{\rm Var}\,(\log L_i/L_\odot) \\ & -2x\,{\rm Covar}\,(\log D_{{\rm mom},i},\, \log L_i/L_\odot) \end{aligned} \tag{7}$$

with

$${\rm Covar}\,(\log D_{{\rm mom},i},\, \log L_i/L_\odot) \approx 4{\rm Var}\,(\log R_i/R_\odot) \tag{8}$$

if we neglect the weak dependence of $R_\star$ on $T_{\rm eff}$.

We consider this type of regression as essential, since the errors in $\log L$ are of the same order as those in $\log D_{\rm mom}$, and they *are* correlated indeed. e.g., if we assume that the momentum rate is lower because of a smaller radius, we also have to assume that the luminosity is smaller (and vice versa), a fact not accounted for in the standard type of regression.

Actually, by comparing with results from a conventional least square fit (even accounting for the specific errors in $\log D_{\rm mom}$), we sometimes find significant differences in the regression coefficients. Only when the errors in $\log L$ are small, both methods yield similar results. Insofar, the more simple method might be justified in cases where the (relative) uncertainty in distance is small, e.g., in investigations of extra-galactic sources or specific associations, as performed by Herrero et al. (2002).

In Fig. 6 one can see that *normal giants and dwarfs show lower wind momenta (roughly by 0.3...0.5 dex) than supergiants at the same bolometric luminosity*, and that they are in good agreement with the theoretical predictions by Vink et al. (2000, dashed line). Note that because of the short interval in $\log L$ covered by giants and dwarfs, the regressions

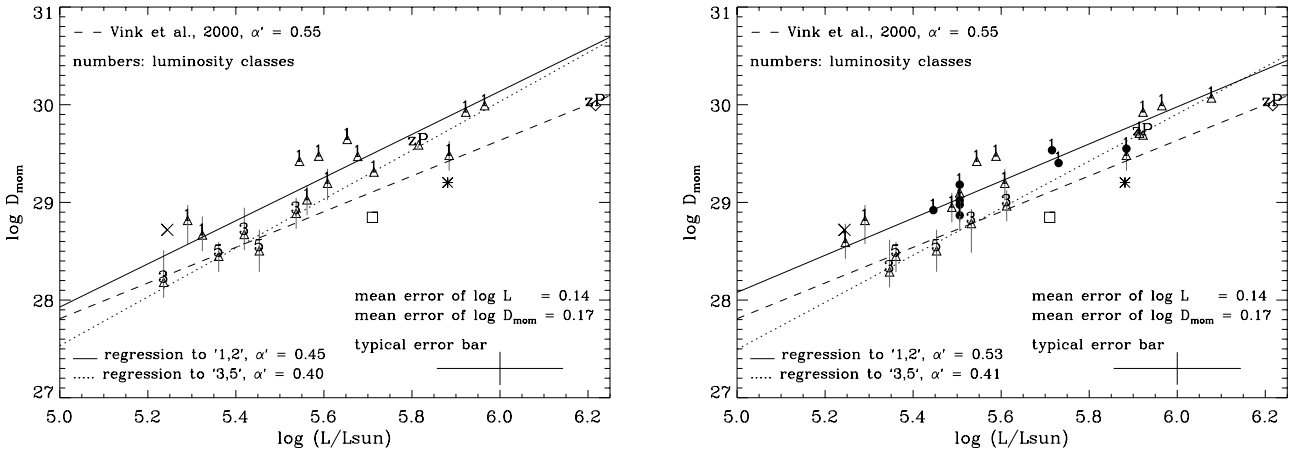

Fig. 6. WLR for our sample of Galactic O-type stars. Case A (*left*) and case D (*right*) as discussed in the text. Error bars with respect to $\Delta \log D_{\rm mom}$ are displayed for all stars with Hα in absorption. The errors for the remaining objects with Hα in emission and the errors for $\Delta \log L$ roughly agree with the typical error bars displayed in the figures. Regressions obtained from χ^2 minimization with individual errors in both co-ordinates, accounting for the covariance between luminosity and modified wind-momentum rate. Numbers 1, 3 and 5 correspond to luminosity classes I, III and V, respectively. Special symbols: "zP" corresponds to ζ Pup as used for the regression (either standard or entry 2) and additionally to entry 4 (upper right). The "x" denotes HD 47 839 (15 Mon, lc V), the open square HD 16 429 (lc I) and the asterisk HD 34 656; all three objects have been discarded from the corresponding regressions. The filled circles denote the field stars of our sample included for case D.

for luminosity III/V objects cannot be regarded as significant. Thus, in Table 4 only the regression coefficients for the luminosity class I objects obtained for the different samples (A, B, C and D) are listed.

There are three stars that deviate strongly from the above "rule": HD 47 839 (15 Mon, denoted by an "x"), HD 16 429 (denoted by an open square) and HD 34 656 (denoted with an asterisk). Interestingly, all these stars have been recognized as "blue stragglers" (Schild & Berthet 1986), among which the rate of double/multiple systems seems to be exceptionally high (Bellazzini et al. 2002; Carney et al. 2001). Actually, the former two objects were proven to be a double (Gies et al. 1993, and references therein) and a triple (Gies, private communication) system, respectively – a result that might explain their "erroneous" position (compared to the theoretical predictions). Accordingly, one might speculate that the excess luminosity of HD 34 656 might also be due to the influence of (a) possible companion(s). In view of these uncertainties, we have discarded all three objects from the regression.

In addition, we like to mention that ζ Pup with parameters from entry (4), i.e., assuming the "large" radius, lies well below the regression of the other lc I objects, whereas with the "conventional" radius its location is just slightly below the mean. This result might be used to favour the lower radius. Note, however, that ζ Pup is a "bona fide" runaway star, i.e., its parent association, Vela R2, has been identified, and hence it is quite probable that the star has not reached its present status through single star evolution. In particular, Vanbeveren et al. (1998) have argued that ζ Pup could not have become a single runaway as a consequence of close encounters with other stars in a very dense cluster, but is more likely to originate from a supernova explosion in a massive close binary. In view of this scenario, the "peculiar" characteristics of ζ Pup, such as enhanced He and N abundances at the stellar surface, higher

Table 4. Coefficients of the WLR obtained for the supergiants of our sample cases A, B, C and D in comparison to results from other investigations. The values of the minimized χ^2 (not displayed here) indicate an acceptable fit in all four cases. Regression accounting for errors in both co-ordinates for case A to D and the analysis by Repolust et al.; standard least square fit for remaining entries.

Sample	$\log D_{\rm o}$	x	α'
Case A	16.88 ± 2.53	2.21 ± 0.45	0.45 ± 0.09
Case B	17.53 ± 2.18	2.10 ± 0.38	0.48 ± 0.09
Case C	19.00 ± 1.37	1.83 ± 0.24	0.55 ± 0.08
Case D	18.58 ± 1.25	1.90 ± 0.22	0.53 ± 0.06
Herrero et al.	19.27 ± 1.37	1.74 ± 0.24	0.58 ± 0.08
Repolust et al.	18.30 ± 2.12	1.97 ± 0.38	0.51 ± 0.10
Kudritzki & Puls	20.69 ± 1.04	1.51 ± 0.18	0.66 ± 0.08
Vink et al. (2000)	18.68 ± 0.26	1.83 ± 0.044	0.55 ± 0.013

peculiar and rotational velocities and overluminosity might all find their natural explanation.

Our analysis indicates that the regression somewhat improves, i.e., the errors of the parameters decrease (and move towards those predicted by theory, cf. Table 4), when individual values of R (case B) are used instead of the standard ones. This improvement becomes even larger by adopting those parameters resulting from a calibration of $M_{\rm V}$ for objects suspected to be runaway stars (Case C). The final inclusion of the definite field stars (lower part of Table 1) has a minor influence on the corresponding regression coefficients (Case D), although the statistics futher improves. Accounting for the fact that the positions of these stars remain somewhat uncertain since they strongly depend on the accuracy of the empirical $M_{\rm V}$-calibration, we will concentrate now on sample C, since it appears to be the most relevant, in terms of both statistics and underlying physical assumptions.

Comparison with other investigations. Apart from the work by RPH mentioned in the introduction, there are a number of other investigations which have previously tried to derive wind-momentum rates as function of luminosity. In particular, Kudritzki & Puls (2000) and Herrero et al. (2002) provided corresponding coefficients for Galactic O-type supergiants, which have been included in Table 4 for comparison. Note that the values quoted by Kudritzki & Puls (2000) refer to the analysis of Puls et al. (1996), i.e., have been derived by means of *unblocked* model atmospheres, and that all coefficients except those from RPH refer to conventional least square fitting. Additionally, we quote the coefficients of the theoretical relation for stars with $T_{\rm eff} > 30\,000$ K as calculated by Vink et al. (2000), which is predicted to be independent of luminosity class (see below) and compares well with the position of our lc III/V objects.

Except for the data from Kudritzki & Puls (2000), the remaining "observational" results are rather similar. On the one hand, this is not too astonishing, since all three investigations either use or rely on the same (line-blanketed) model atmosphere code, FastWind. On the other hand, however, the fairly good agreement between our results (in particular, Case D) and those from the complete spectral analysis (RPH) indicates that the approximate approach followed by us actually can provide compatible results in terms of both mass-loss rates (Sect. 4.3) and WLR, not only qualitatively, but also quantitatively.

5.2. Enlarging the sample

The latter conclusion allows us to proceed in the spirit as outlined in the introduction, namely to combine our data with the data-sets from RPH for stars not in common and Herrero et al. (2002), in order to improve the statistics and to study the WLR of Galactic O stars by means of the largest sample of stars used so far. In total, this sample comprises 19 supergiants and 15 lc III/V objects entering the regression. Again, we have accounted for the errors in both directions, with errors taken from the respective investigations. Note that the errors in the sample from Repolust et al. are dominated by the uncertainty in radius, similar to the objects from our sample. In contrast, the errors in the sample from Herrero et al. are somewhat lower, since these authors have investigated objects from *one* association only, i.e. CygOB2, which reduces the scatter.

The results obtained in Fig. 7 confirm those presented in the previous section as well as the ones reported by RPH: the WLR for luminosity class III/V objects strictly follows the theoretical predictions while the relation for the supergiants shows a vertical offset, corresponding now to an average factor of roughly 0.25 dex.

Note that with respect to lc III/V objects, the "unified" sample covers a much larger range in $\log L$. Thus a more precise determination of the corresponding regression coefficients than before is possible. Note in addition that even those stars with only upper limits for $D_{\rm mom}$ (those with an arrow), which have *not* been included into the regression, follow the continuation of lc III/V objects – a finding that has already been discussed by RPH.

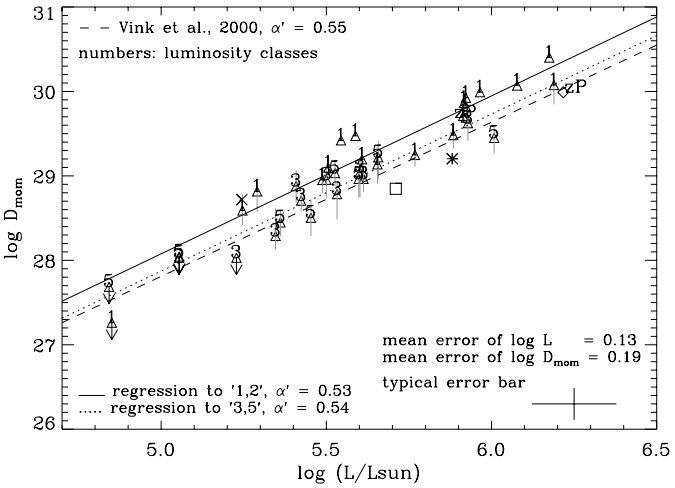

Fig. 7. WLR for Galactic O-type stars. Sample includes our sample case C, the sample by RPH for objects *not* in common and the sample by Herrero et al. (2002). Regression accounting for errors in both directions and appropriate correlations; errors corresponding to respective publications. All symbols as in Fig. 6; arrows indicate upper limits for objects with almost purely photospheric profiles which have been discarded from the regression.

Table 5. Coefficients of the WLR obtained for Galactic O-stars, by combining our sample case C with the results from Herrero et al. (2002) and RPH for objects not in common. Regression accounting for errors in both co-ordinates. $\chi^2/(N-2)$ gives the "average" value of the minimized χ^2 per degree of freedom, when N is the number of objects included in the sample. "lc" denotes regression as function of luminosity class, "pt" as function of profile type, respectively. Asterisks mark corresponding data from RPH.

Sample	$\log D_{\rm o}$	x	α'	$\chi^2/(N-2)$
lc I	18.73 ± 1.13	1.87 ± 0.20	0.53 ± 0.06	0.77
lc I*	18.24 ± 1.76	1.96 ± 0.30	0.51 ± 0.08	
lc III/V	18.57 ± 1.98	1.86 ± 0.36	0.54 ± 0.10	0.66
lc III/V*	18.64 ± 1.29	1.85 ± 0.23	0.54 ± 0.07	
pt 1	19.75 ± 1.85	1.71 ± 0.32	0.58 ± 0.11	0.50
pt 3	19.28 ± 1.15	1.74 ± 0.21	0.57 ± 0.07	0.64

The results of the regression analysis for our "unified" sample and for the "unified" sample of RPH are summarized in Table 5. Note in particular that the coefficients for lc I objects derived by us are closer to the values predicted by theory and affected by smaller errors (due to the improved statistics) than those obtained by RPH. Note also that because of the inclusion of giants and dwarfs from our investigation, the "unified" lc III/V sample now shows a better coverage along the $\log L$ axis (with no gaps in between). The corresponding regression coefficients, however, deviate stronger from the values predicted by theory and have a somewhat larger error than those derived by RPH. This finding (for weak winds) again points to the β problem discussed in Sect. 4.3 and may also indicate a higher sensitivity of the results on the approximations used by our method.

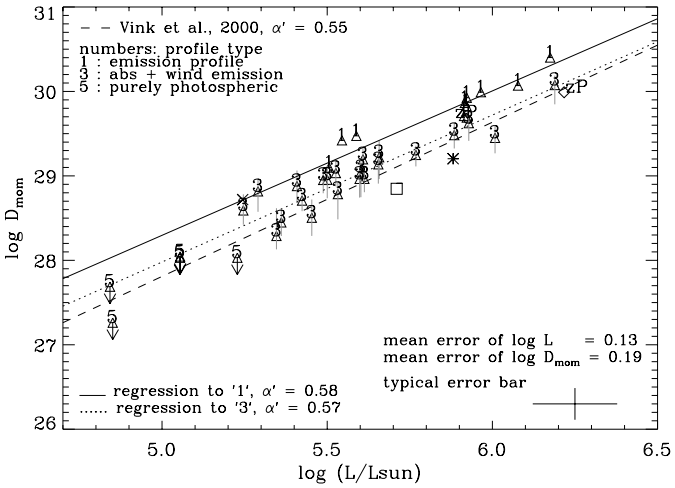

Fig. 8. As Fig. 7, but with regression in dependence of profile type (see text).

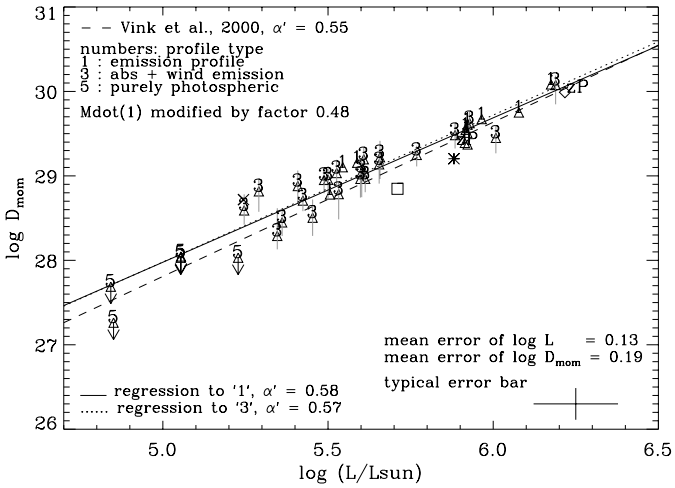

Fig. 9. As Fig. 8; $\dot{M}$ of class 1 objects (Hα in emission) decreased by a factor of 0.48.

5.3. WLR as function of profile type

The clear separation between the WLRs for luminosity class I objects and those of luminosity class III/V might in principle be explained by a different number of effective lines driving the wind, since the coefficient $D_{\rm o}$ depends on this quantity via $D_{\rm o} \propto N_0^{1/\alpha'}$ (cf. Kudritzki & Puls 2000, their Eq. (18)). However, such a difference is rather unlikely since present theoretical simulations of line-driven winds (on the basis of completely different approaches) do not find such a separation, but predict a unique relation instead (Vink et al. 2000; Pauldrach et al. 2002; Puls et al. 2003).

Although the separation between supergiants and the rest is fairly obvious, there are certain outliers that are much more consistent with the regression for lc III/V stars. Among them are three supergiants from the sample of Herrero et al. with well-defined positions due to their membership to CygOB2. Interestingly, all these outliers show Hα in absorption. Note that this confusing situation has already been noted by Puls et al. (2003).

Subsequently, these authors suggested to plot the WLR in a slightly different manner, namely as a function of profile type instead of luminosity class. Class 1 corresponds to objects with Hα in emission, class 3 to objects with Hα in absorption and class 5 to objects with an almost purely photospheric profile, i.e., with very thin winds. In this way, these authors found a much closer correlation without any outliers.

In Fig. 8, we have repeated this exercise for our "unified" sample. The corresponding coefficients are displayed in Table 5. Our conclusion for the enlarged sample is not as clear as for the data used by Puls et al. (2003), but similar to that reported by RPH. In fact, the situation for emission type objects has improved, and the fit quality (expressed by the minimized χ^2) for class 1 objects is lower than for lc I objects. Also, for class 3 objects the scatter in the regression coefficients has decreased compared to lc III stars. A closer inspection of Fig. 8, however, reveals a new problem: At $\log L/L_\odot < 5.4$, we find at least two class 3 stars located considerably above the corresponding regression curve.

Both of these objects are supergiants, HD 18 409 and HD 207 198; neither of them is a fast rotator or suspected binary. Certainly one could find reasons to exclude them from the regression, but we regard their positions as reliable within the error bars. Although there are certain discrepancies with respect to the derived Q-values (cf. Sect. 4.3), they cover similar positions in the investigation by Repolust et al., i.e., they lie in the continuation of class 1 stars.

Thus, we encounter the following situation: at larger luminosities, $\log L/L_\odot > 5.5$, the *separation* of the WLR seems to be more a function of profile type than of luminosity class (which might indicate that the present classification scheme is simply too coarse). For lower luminosities, the opposite might be true, or the clear relationship between $D_{\rm mom}$ and $\log L$ vanishes at all. Before a final statement can be given, however, a complete NLTE analysis has to be awaited for, at least for the critical objects with low momentum rates, since in this case the errors bars are particularly large.

Following the suggestion of Puls et al. (2003, see also RPH) that there might be no separation at all, but that for objects with emission lines one observes the effects of clumping[2], we shifted the WLR of class 1 stars onto the WLR for class 3 stars by reducing $\dot{M}$ by a factor of 0.48 (cf. Fig. 9). The corresponding (effective) clumping factor equals 4.3 ($< \rho^2 > / < \rho >^2 = 0.48^{-2}$)

6. Summary, discussion and conclusions

The first objective of the present paper was to investigate the potential of a pure Hα profile analysis to provide mass-loss and wind-momentum rates for O-type stars, compatible to those from a state-of-the-art complete spectral analysis. This goal has been attained in two ways: (i) by comparing the derived mass-loss rates (actually, the corresponding Q-values) to those determined by RPH via a complete NLTE spectral analysis for stars in common and (ii) by comparing the Wind-momentum

[2] This mimics a higher mass-loss rate than actually present, in analogy to the case of WR-stars, cf. also Sect. 1.

Luminosity Relationship for our sample stars to those derived by other investigators (Kudritzki & Puls 2000; Herrero et al. 2002, RPH) Additionally, we studied the consequences of "fine tuning" direct and indirect parameters entering the WLR, e.g., by taking different values for stellar reddening and distance into account.

To determine $\dot{M}$ and velocity field exponents β, we applied the approximate method developed by Puls et al. (1996) which has been modified by us to account for the effects of metal line-blocking/blanketing. Effective temperatures and gravities needed to perform the Hα profile fitting have been obtained via spectral type – $T_{\rm eff}$ and spectral type – $\log g$ calibrations for O stars of luminosity classes I, III and V. These calibrations are based on results of recent spectroscopic analyses of individual Galactic stars derived via NLTE atmospheric models with mass-loss, sphericity and metal line blocking/blanketing (RPH; Martins et al. 2002).

It must be noted that in our regression we have assumed a linear relation between spectral type and $T_{\rm eff}$, a fact that might raise some suspicion concerning the reliability of the derived temperatures (see, e.g., Crowther 1998). Note, however, that the data underlying our calibrations did not give any evidence of significant deviations from a linear approach. This is particulary true for the case of dwarfs and supergiants where the available data cover a relatively wide range of subclasses. Admittedly, at spectral types earlier than O5 our calibration for luminosity class III might be somewhat unrealistic due to the lack of appropriate data. However, since our sample does not comprise any objects in this range, our analysis is not affected by this uncertainty. One word of warning: caution is well-advised when using the provided calibrations for supergiants, since they refer to "typical" representatives as considered in the present investigation, but *not* to extreme objects. In the latter case (which is visible, e.g., from the strength of the Hα line itself), the uniqueness of a spectral type – $T_{\rm eff}$ relation is no longer guaranteed.

On the basis of these calibrations, we have analyzed Hα by means of the approximate method cited above. The major modification to include the effects of line-blanketing concerns the change of radiation temperature in the neighbouring continuum. A comparison of our Q-values with those from RPH (see above) for 11 stars in common indicates that both methods give excellent agreement in those cases where the wind-emission is significant, whereas for (very) low wind-densities discrepancies may arise, which are mostly related to the problem of uncertain velocity exponents, β.

Based on the complete set of stellar and wind parameters we derived the corresponding WLR for the sample stars accounting for different combinations of stellar reddening and distances available in the literature. In particular, this analysis indicates that using individual instead of mean values for stellar reddening causes variations in $\log L$ and $D_{\rm mom}$, which are (much) smaller than the individual uncertainties for these quantities.

Our analysis showed that not only the Q-values but also the WLR derived by means of our approximate approach are in good agreement to the results originating from a complete spectral analysis. In particular, we confirm the result published by RPH that the WLR for lc III/V strictly follows the theoretical predictions of Vink et al. (2000), while the relation for lc I shows a vertical offset.

Following the idea of Puls et al. (2003), this offset may reflect the effects of clumping in the innermost part of the wind. For the combination of our sample with data from comparable investigations, we find that with an enhancement factor of $\sim$2 for stars with Hα in emission the differences in the corresponding WLRs almost vanish and a unique relation can be obtained (though some problems at lower luminosities still exist admittedly). This enhancement factor corresponds to an effective clumping factor of 4.3, which is somewhat lower than in WR winds and in agreement with the value provided by RPH.

The possibility to use the WLR as an indicator of wind clumping in O-star winds is very exciting but needs to be proven independently. One way to check this possibility is to compare Hα and radio mass-loss rates. In case both the suggested radial stratification of the clumping factor (Owocki et al. 2000), and the assumption made by Puls et al. were correct, one might expect larger Hα mass-loss rates for stars with stronger winds, i.e. Hα in emission, whereas the opposite, i.e., similar or even higher radio mass-loss rates, might be expected for stars with weaker winds (Hα in absorption). Guided by this perspective we compared mass-loss rates derived from Hα with such derived from radio free – free emission (Lamers & Leitherer 1993; Scuderi et al. 1998) for stars in common. In total, these are seven stars, but only for four stars we have information concerning the distance (for the other three we have calibrated $M_{\rm V}$): HD 190 429A, HD 66 811, HD 192 639 and HD 36 861. The results obtained indicate perfect agreement between the $\dot{M}$-estimates for the lc III star HD 36 861 with Hα in absorption ($\log \dot{M}\,({\rm H}\alpha)\,/\dot{M}\,({\rm radio}) = 0.03$), while for the three supergiants with Hα in emission the radio mass-loss rates are lower than those from Hα (by an average factor of $\sim$2). In particular, we found $\log \dot{M}\,({\rm H}\alpha)\,/\dot{M}\,({\rm radio})$ equal to 0.29 for HD 190 429 (d = 2.3 kpc), equal to 0.36 for HD 192 639 (d = 1.82 kpc) and equal to 0.40 for HD 66 811 (d = 0.7 kpc). This finding is thus consistent with both the presence of a stratified clumping factor and our assumption that clumping is "observable" only in the Hα emission of stronger winds.

The results outlined above indicate that the approximate method employed can provide results which are not only quantitatively but also qualitatively consistent to those from a complete spectral analysis. Therefore, this method can be used to solve the statistical problem mentioned in the introduction when studying wind properties of Galactic O-stars and especially when addressing the problem of wind clumping by comparing optical and radio observations. Note in particular that the *ratio* of Hα and radio mass-loss rate remains almost unaffected by any uncertainty in distance, if both values are derived using the *same* value for d: since both mass-loss rates (as function of Q and of flux, respectively) depend on $d^{-1.5}$, the distance cancels almost out, except for the effects of reddening. This means that field stars can also be used as targets for studying wind clumping, a fact that will allow to additionally improve the statistics.

Although the uncertainties in distance cause many problems when studying radii and wind parameters of Galactic

stars, we finally like to emphasize that we cannot refrain from such an investigation because of the need to establish a reference base for the behaviour of stars with the corresponding metallicity.

6.1. Future work

While considerable progress has been obtained with respect to the WLR for (Galactic) O-type stars, also a number of questions became evident. In our opinion, one of the most important problems is the following: Presently, we do not know (at least with confidence) the Hα-wind-momentum rates of low luminosity supergiants ($\log L/L_{\odot} < 5.5$) due to the lack of a significant number of objects in our present sample. In particular, for objects with Hα in absorption we have to answer the question whether the momentum rate is similar or higher than theoretically predicted[3].

In the former case our assumption concerning the behaviour of Hα ("actual" $\dot{M}$, if profile in absorption) still works, while in the latter case it becomes questionable. To clarify this point we have started a new observational program that focuses on lc I objects with $\log\ L \leq 5.5$. The question concerning the behaviour of B and A supergiants is obvious, and should also be answered in a follow-up investigation.

Even if there is clumping, the question concerning its radial stratification still remains and introduces a number of additional parameters concerning the model atmospheres. The only way to derive reliable constraints is via a multi-wavelength campaign, where the radio and IR domain are particularly important, since the effective stellar radius (i.e., the region where the optical depth reaches unity) is increasing with wavelength. In this regard and as a next step, we plan to perform and analyze radio observations at least for those stars of our sample which can be detected at radio wavelengths.

Acknowledgements. We like to thank our anonymous referee for very useful suggestions and comments. N.M. highly appreciates financial support from the German DFG under grants 436 BUL 112/21/01 and 436 BUL 112/34/02. TR gratefully acknowledges financial support in form of a grant by the International Max- Planck Research School on Astrophysics (IMPRS), Garching. This work is supported in part by NSF to MES (Bulgaria) through grant F-813/98.

References

Abbott, D. C., Bieging, J. H., & Churchwell, E. 1981, ApJ, 250, 645
Barbier-Brossat, M., & Figon, P. 2000, A&AS, 142, 217
Bellazzini, M., Fusi Pecci, F., Messineo, M., et al. 2002, AJ, 123, 1509
Bianchi, L., & Garcia, M. 2002, ApJ, 581, 610
Cardelli, J. A. 1988, ApJ 335, 177
Cardelli, J. A., Clayton, G. C., & Mathis, J. C. 1989 ApJ, 345, 245
Clayton, G. C., & Cardelli, J. A. 1988, AJ, 96, 695
Carney, B. W., Latham, D. W., & Laird, J. B., et al. 2001, AJ, 122, 3419
Conti, P. S., Leep, E. M., & Lorre, J. J. 1977, ApJ, 214, 759
Crowther, P. A. 1998, ed. T. R. Bedding, A. J. Booth & J. Davis (Dordrecht: Kluwer), Proc. IAU Symp., 189 , 137
Crowther, P. A., Hillier, D. J., Evans, C. J., et al. 2002, ApJ, 579, 774
Crowther, P. A., Hillier, D. J., Fullerton, A. W., et al. 2001, A&AS 199, 130
Cruz-Gonzalez, C., Recillaz-Cruz, E., Costero, R., et al. 1974, Rev. Mex. Astron. Astrofis., 1, 211
Eversberg, Th., Lepine, S., & Moffat, A. F. J. 1998, ApJ, 494, 799
Feldmeier, A. 1995, A&A, 299, 523
Feldmeier, A., Pauldrach, A., & Puls, J. 1997, A&A, 322, 878
Felli, M., Habing, H. J., & Israel, F. P. 1977, A&A, 59, 43
FitzGerald, M. P. 1970, A&A, 4, 234
Garmany, C. D., & Stencel, R. E. 1992, A&AS, 94, 221
Gies, D. R. 1987, ApJS, 64, 545
Gies, D. R., & Bolton, C. T. 1986, ApJS, 61, 419
Gies, D. R., Mason, B. D., Hartkopf, W. I., et al. 1993, AJ, 106, 2027
Groenewegen, M. A. T., & Lamers, H. J. G. M. L. 1989, A&AS, 79, 359
Groenewegen, M. A. T., Lamers, H. J. G. M. L., & Pauldrach, A. W. A. 1989, A&A, 221, 78
Haser, S. M. 1995, Ph.D. Thesis, University of Munich
Herrero, A., Kudritzki, R.-P., Vilchez, J. M., et al. 1992, A&A, 261, 209
Herrero, A., Puls, J. , & Najarro, F. 2002, A&A, 396, 949
Hillier, D. J., Miller, D. L. 1998, ApJ, 496, 407
Hiltner, W. A. 1956, ApJS 2, 389
Hiltner, W. A., & Iriarte, B. 1955, ApJ, 122, 185
Howarth, I. D., & Prinja, R. K. 1989, ApJS, 69, 527
Howarth, I. D., Siebert, K. W., & Hussain, G. A., et al. 1997, MNRAS, 284, 265
Hubeny, I., & Lanz, T. 1995, ApJ 39, 875
Humphreys, R. 1978, ApJS, 38, 309
Kudritzki, R.-P. 1980, A&A, 85, 174
Kudritzki, R.-P., & Puls, J. 2000, ARA&A, 38, 613
Lamers, H. J. G. M. L., & Leitherer, C. 1993, ApJ, 412, 771
Lamers, H. J. G. M. L., Snow, T., & Lindholm, D. M. 1995, ApJ, 455, 269
Lamers, H. J. G. M. L., Haser, S., de Koter, A., et al. 1999, ApJ, 516, 872
Lennon, D.J., Dufton, P. L., & Fitzsimmons, A. 1992, A&AS, 94, 569
Markova, N., & Scuderi, S. 2003, A&A, in prep.
Markova, N., Valchev, T. 2000, A&A, 363, 995
Martins, F., Schaerer, D., & Hillier, D. J. 2002, A&A, 382, 999
Massa, D., Fullerton, A. W., Sonneborn, G., et al. 2003, ApJ, 586, 996
Meynet, D., Maeder, A., Schaller, G., et al. 1994, A&AS, 103,97
Moffat, A. F. J., & Robert, C. 1994, ApJ, 421, 310
Nelan, E., et. al. 2003, in prep.
Owocki, S. P., & Puls, J. 1999, ApJ, 510, 355
Owocki, S. P., Castor, J. I., & Rybicki, G. B. 1988, ApJ, 335, 914
Owocki, S. P., Runacres, M. C., & Cohen, D. H. 2000, in Thermal and Ionization Aspects of Flows from Hot Stars: Observations and Theory, ed. H. J. G. L. M. Lamers & A. Sapar, ASP Conf. Ser., 204, 183
Pauldrach, A. W. A., Hoffmann, T. L., & Lennon, M. 2001, A&A, 375, 161
Pauldrach, A. W. A., Hoffmann, T. L., & Mendéz, R. H. 2002, in Proc. IAU Symp. 209, ed. S. Kwok & M. Dopita, in press
Penny, L. R. 1996, ApJ, 463, 737
Puls, J., Kudritzki, R.-P., Herrero, A., et al. 1996, A&A, 305, 171
Puls, J., Springmann, U., & Lennon, M. 2000, A&AS, 141, 23
Puls, J., Repolust, T., Hofmann, T., et al. 2002, in Proc. IAU Symp. 212, ed. K.A. van der Hucht, A. Herrero & C. Esteban, ASP Conf. Ser, 61
Press, W. H., Teukolsky, S. A., Vetterling, W. T., et al. 1992, Numerical Recipes in Fortran, 2nd edition (Cambridge University Press)

[3] Remember that for the only two supergiants at low L in our sample we found higher values, however not at a statistically significant level.

Repolust, T., Puls, J., & Herrero, A. 2003, A&A, accepted, "RPH"
Sahu, M., & Blaauw, A. 1993, in Massive Stars: Their Lives in the Interstellar Medium, ed. J. P. Cassinelli & E. B. Churchwell, ASP Conf. Ser., 35, 278
Schild, H., & Berthet, S. 1986, A&A 162, 369
Scuderi, S., & Panagia, N. 2000, in Termal and Ionization Aspects of Flows from Hot Stars: Observations and Theory, ed. H. J. G. L. M. Lamers & A. Sapar, ASP Conf. Ser., 204, 419
Scuderi, S., Panagia, N., Stanghellini, C., et al. 1998, A&A, 332, 251
Scuderi, S., Panagia, N., Stanghellini, C., et al. 2003, A&A, in prep.
Stone, R.C. 1979, ApJ, 232, 520
Tovmassian, H. M., Hovhannessian, R. Kh., Epremian, R. A., et al. 1994, MNRAS, 266, 337
Vacca, W. D., Garmany, C. D., & Shull, J. M. 1996, ApJ, 460, 914
Vanbeveren, D., de Loore, C., & van Rensbergen, W. 1998, A&ARv, 9, 63
Vink, J. S., de Koter, A., & Lamers, H. J. G. L. M. 2000, A&A, 362, 295
Wegner, W. 1994, MNRAS, 270, 229
Walborn, N. R. 1971, ApJS, 23, 257
Walborn, N. R. 1972, AJ, 77, 312
Walborn, N. R. 1973, AJ, 78, 1067
Walborn, N. R. 2002, AJ, 124, 507
Woosley, S. E., Heger, E., & Weaver, T. A. 2002, Rev. Mod. Phys., 74, 1015